Interrogation technique for TFBG-SPR refractometers based on differential orthogonal light states

Valérie Voisin,[1,*] Christophe Caucheteur,[1] Patrice Mégret,[1] and Jacques Albert[2]

[1]Electromagnetism and Telecommunication Department, Université de Mons, Place du Parc 20, 7000 Mons, Belgium

[2]Department of Electronics, Carleton University, 1125 Colonel By Drive, K1S 5B6 Ottawa, Canada

*Corresponding author: valerie.voisin@umons.ac.be

Received 19 May 2011; accepted 16 June 2011;
posted 27 June 2011 (Doc. ID 147671); published 21 July 2011

The generation of near-IR surface plasmon resonance in gold-coated tilted fiber Bragg gratings is strongly dependent on both the polarization state of the transmission light and the property of confining materials (including the coating materials and surrounding media). These dependencies can be advantageously used to demodulate the amplitude spectrum and retrieve the surrounding refractive index. In this paper, we present an automated demodulation technique that measures the surrounding refractive index by comparing the differential amplitude of resonance peaks near the plasmon attenuation for two orthogonal amplitude spectra recorded in the same operating conditions. A mean sensitivity of more than 500 nm per refractive index unit is reported. This new refractive index measurement method is shown to be accurate to 5×10^{-5} over a full range of 0.01 in water solutions. © 2011 Optical Society of America

OCIS codes: 060.2370, 240.6680.

1. Introduction

The field of refractometry is wide and it covers important applications in the chemical and food industry, environmental control, or medical analysis. For some of these applications, a miniature and therefore minimally invasive sensor would be very beneficial. So, fiber-optic-based refractometers were developed during the past few years as, thanks to their small dimensions and remote operation, they present decisive advantages over traditional prism-based transducers. To obtain an accurate measurement of the surrounding refractive index (SRI) changes with an optical fiber sensor, the guided light has to be brought into contact with the surrounding medium of the fiber. Hence, fiber gratings that couple light from the core toward the surrounding medium are privileged over misaligned splice or etched fiber regions as they keep the fiber integrity [1,2]. In this work, we use tilted fiber Bragg gratings (TFBGs), which have been demonstrated to be accurate fiber-optic refractometers, allowing remote detection in very small volumes [3]. Moreover, unlike long period fiber gratings, TFBGs provide temperature-insensitive measurements [4,5].

A TFBG is a short-period grating tilted by a certain angle with respect to the fiber axis. The typical TFBG transmitted spectrum is composed by resonances at different wavelengths. The longest wavelength is called the Bragg wavelength (λ_{Bragg}) and corresponds to the coupling between the co- and contra-propagating core modes. Other resonances result from the coupling between the core mode and contra-propagating cladding modes of the fiber. Cladding modes propagate near the cladding-external medium interface yielding a TFBG amplitude spectrum sensitive to the SRI [6].

To retrieve the SRI from the TFBG amplitude spectrum, two main demodulation techniques have been proposed. The first method is a global technique that consists in measuring the area delimited by

0003-6935/11/224257-05$15.00/0

the cladding modes in the TFBG transmitted amplitude spectrum [3]. The second method consists in measuring selective cladding mode resonance shifts relative to the core mode resonance, as the spacing between the Bragg wavelength and a cladding mode resonance yields temperature-sensitive SRI measurements [4]. Besides these techniques, another method is a power-referenced detection based on the measurement of the normalized TFBG transmitted power [7]. These methods offer a good repeatability and allow to know the SRI with an accuracy of the order of 10^{-4}.

To improve the sensitivity to the SRI, a nanoscale gold coating has been deposited on TFBGs. Thanks to this nanoscale gold coating, the generation of surface plasmon resonances (SPRs) can occur. Indeed, the nonzero evanescent fields of the cladding modes extend outside the cladding and hence into the metal film. When the effective refractive index and the polarization state of the cladding modes are equal to those of the plasmon wave, there is a transfer of energy to a plasmon wave across the metallic surface. The advantage of the TFBG is that it excites tens to a hundred of cladding modes, which is equivalent to optical rays hitting the cladding-metal interface with different angles of incidence, ensuring excitation of the SPR at some particular wavelengths. The usefulness of gold-coated TFBGs was demonstrated for accurate refractometric purposes [8], opening the way to *in situ* biosensing.

Recently, it was demonstrated that light polarization plays a crucial role not only in the generation of SPRs but also in the subsequent amplitude spectrum demodulation [9–13]. The use of two particular orthogonal polarization light states (maximizing and minimizing the SPR signature in the amplitude spectrum) automates the demodulation technique and improves its sensitivity to the SRI [14,15]. In these works, the unique signature of the TFBG polarization dependent loss spectrum was exploited to achieve a minimum detection level of 1×10^{-5} over a range of 10^{-4} in SRI. We propose here an alternative methodology that is simpler to automate and that provides a direct measurement of the SRI across a wide range of values without ambiguity and without loss of resolution. This method is based on the computation of the wavelength and amplitude between corresponding resonance peaks for both orthogonal amplitude spectra. In addition, it yields important insight about the particular behavior of orthogonal polarization modes with respect to the SRI. The details of the method are given in section 2. Section 3 presents the results obtained using that particular technique.

2. Experiments

Our experiments were conducted with the setup presented in Fig. 1. The sensor is composed of a 1 cm long TFBG characterized by an internal tilt angle equal to 10° and written into hydrogen-loaded single-mode fiber using a pulsed excimer laser

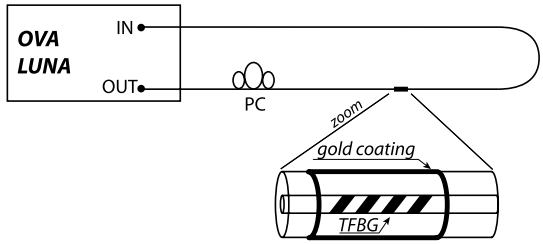

Fig. 1. Sketch of the demodulation technique used to interrogate SPR sensor.

emitting at 248 nm. The TFBG is covered by a 50 nm gold coating deposited by a sputtering process to create a TFBG-SPR refractometer. The deposition is made in two steps. Firstly, a gold deposition is performed with the fiber placed horizontally above the target. Secondly, we operate a rotation of 180° of the fiber along its axis for another deposition in the same operating conditions as the first one. The fiber orientation was carefully positioned in the sputtering chamber to ensure that the tilt plane intersects the regions of higher gold thickness facing the sputtering source.

The amplitude spectrum of the TFBG is collected by an optical vector analyzer (OVA) from *Luna Technologies* offering a measurement resolution of 1.25 pm. A linear polarizer is placed between the OVA optical source (OUT) and the TFBG-SPR sensor to modify the polarization state of the incident light launched into the refractometer. The TFBG-SPR sensor was immersed in a water-salt mixture that we dilute during the experiment to modify its refractive index. The changes in SRI value are calculated on the basis of the added volume and the temperature of the mixture. The latter were measured with an accuracy of 0.1 ml and 0.1 °C, respectively, to control the refractive index changes with high precision. During the experiment, a maximum variation of about 0.5 °C was measured, which was confirmed by a shift of λ_{Bragg} in a range of 5 pm (λ_{Bragg} shifts by ~10 pm/°C). This temperature variation impacts the SRI determination. Since all resonances shift by the same amount under temperature change [4], we have used the Bragg wavelength as a reference to correct the SRI values from the impact of temperature variations. As a result, we get a nominal refractive index uncertainty equal to 1.2×10^{-5} RIU [16].

The setup is used to set orthogonal light states and obtain both specific orthogonal amplitude spectra required for the demodulation step. These two orthogonal states of polarization are the ones for which the SPR is maximized (polarization state x) and minimized (polarization state y). Their amplitude spectra are depicted in Fig. 2 for two different SRI values at the ends of the investigated range. During our experiments, we have measured the evolution of the amplitude spectrum for both polarization states and for different SRI values. As we can see in Fig. 3(a), the amplitude and the wavelength of the cladding mode resonances for the polarization state x vary significantly with an SRI modification (Δn) of ~10^{-2}.

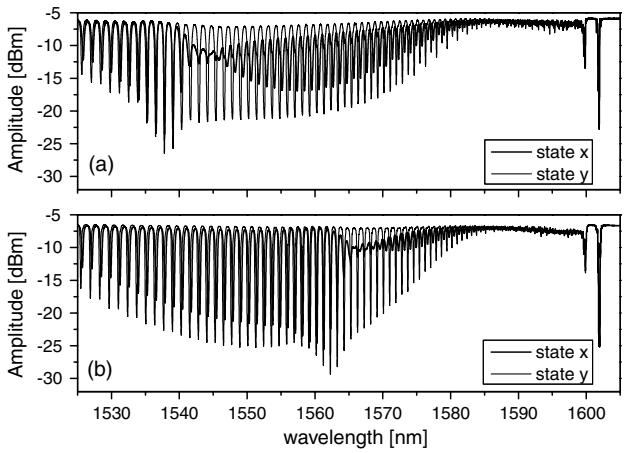

Fig. 2. Orthogonal transmitted amplitude spectra with SPR signature maximized (state x) and minimized (state y) for the refractive index of (a) ~1.33 and (b) ~1.39 (n_{ref}).

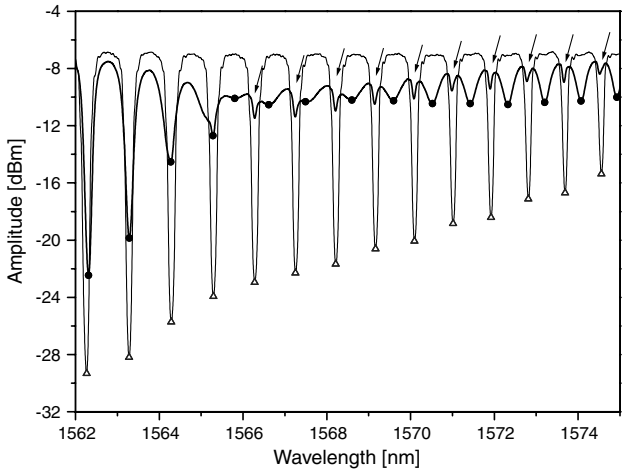

Fig. 4. Zoom on the plasmon resonance with cladding mode resonances detection (dots in x spectrum and triangles in y spectrum).

For the orthogonal polarization, the behavior is opposite as the amplitude and wavelengths of the cladding mode resonances remain quasi unaltered by small SRI changes [see Fig. 3(b)]. These particular observations led us to study the differential amplitudes and wavelength of corresponding (adjacent) cladding mode resonances in the two spectra. In order to do this, an algorithm has been implemented to automatically detect the cladding mode resonances both in amplitude and in wavelength for the two spectra. The resonance peaks detected in the x and y amplitude spectra are respectively indicated by dots and triangles in Fig. 4. This figure shows the critical region around the SPR signature where care was taken to ensure a proper detection of the cladding mode peaks. Note that the algorithm is able to differentiate local extrema corresponding to cladding modes resonances in the x spectra from residual y modes indicated by an arrow in Fig. 4. Indeed, we noted that these parasitic peaks appear all on the right of the SPR signature and that their wavelengths coincide with the wavelengths of the cladding mode resonances observed in the orthogonal polarization state y spectrum. These particularities allow us to filter them out of the interrogation algorithm and to keep only the significant resonances.

3. Results and Discussion

From the detection of the resonance peaks described in Section 2, we compute the differential wavelength ($\Delta\lambda_{x,y}$) and amplitude ($\Delta A_{x,y}$) between two corresponding minima of the x and y amplitude spectra (one dot and one triangle). To reduce the ripple caused by the high resolution measurement, we operate a smoothing (adjacent averaging) of the raw data. Each point of the evolution is equal to the averaging of seven adjacent samples around its position. The results of the computation are given as a function of the wavelength and for different SRI values in Fig. 5 and 6.

We observe that the differential wavelength evolution is discontinuous near the SPR. The position of the discontinuity changes with the SRI and reflects the SPR signature. For an SRI variation of 10^{-2}, we

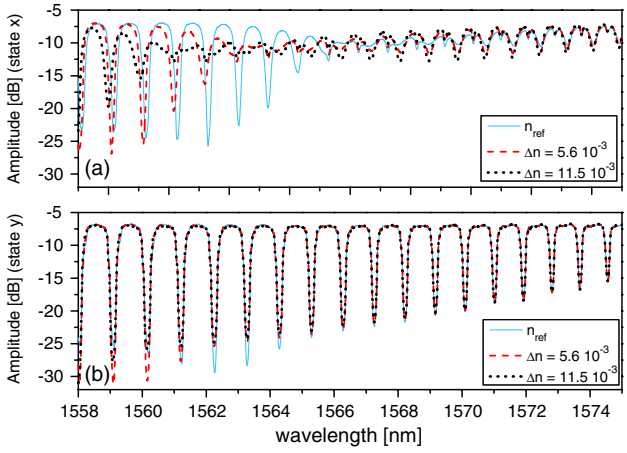

Fig. 3. (Color online) Evolution of transmitted amplitude spectrum (a) for the polarization state x and (b) for the polarization state y as a function of Δn.

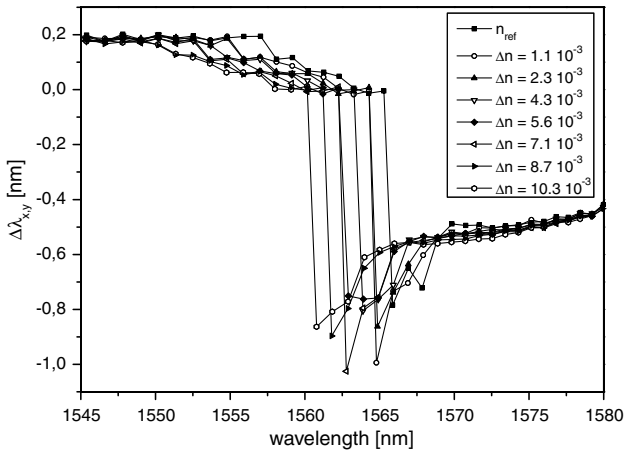

Fig. 5. Differential wavelength of corresponding cladding mode resonances for two orthogonal polarization states as a function of the wavelength.

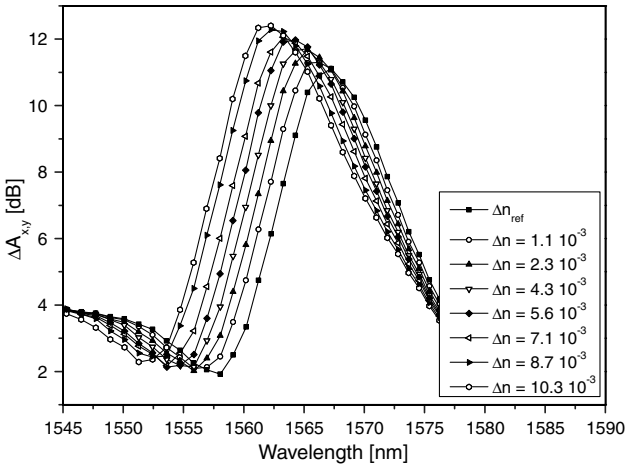

Fig. 6. Differential amplitude of corresponding cladding mode resonances for two orthogonal polarization states as a function of the wavelength.

get a total shift of ~5 nm. However, this shift is not linear because there is a superposition of several differential wavelength curves obtained for different SRI changes of the order of 10^{-3}. We believe that this particular behavior can be attributed to the fact that resonances at the SPR peak are too attenuated and broadened to allow a measurement of the resonance position that has the necessary accuracy to resolve picometer level wavelength shifts as previously indicated in some of early experimental investigations [9,14]. By consequence, we are not able to retrieve the SRI with an efficient accuracy using only $\Delta\lambda_{x,y}$. In contrast, the differential amplitude curves shift linearly and smoothly with the SRI. The total shift observed is about 6 nm for an SRI variation of 10^{-2}. Figure 7 is a zoom on the evolution of $\Delta A_{x,y}$ for different SRI changes around 1560 nm. This figure illustrates the method followed to retrieve SRI. We track the wavelength for which $\Delta A_{x,y}$ is equal to 8 dB (value corresponding to the middle of the transition zone). These corresponding wavelengths are presented as a function of SRI changes in Fig. 8. The response is linear and we obtain a mean SRI sensitivity of 535 nm/RIU (refractive index unit)

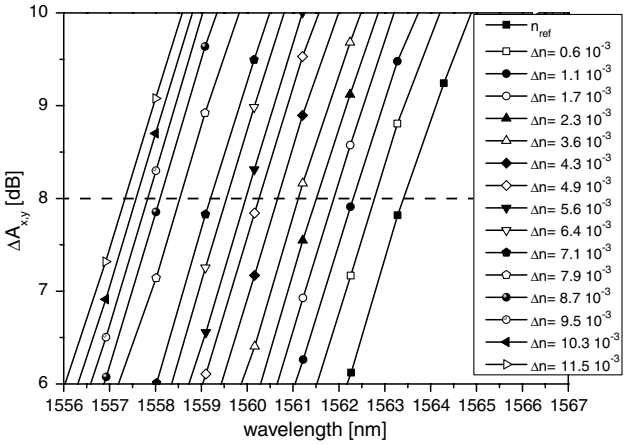

Fig. 7. Evolution of $\Delta A_{x,y}$ around 1560 nm as a function of the SRI (Δn) and its detection threshold ($\Delta A_{x,y} = 8$ dB).

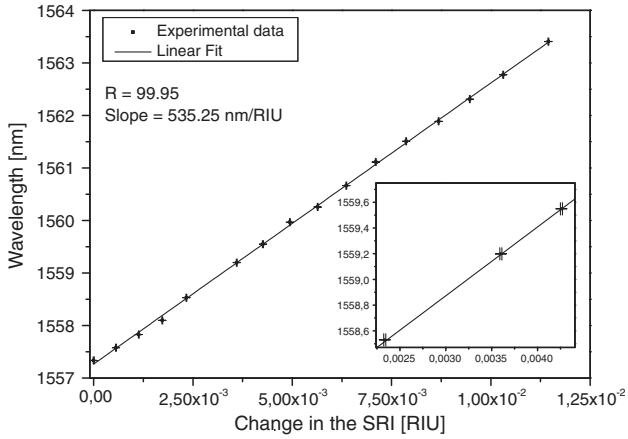

Fig. 8. Wavelength shift of $\Delta A_{x,y}$ as a function of the SRI (Δn). Inset: zoom around $\Delta n = 3.5 \times 10^{-3}$ to better identify the error bars.

with a high correlation (99.95%). Other detection thresholds from 4.5 dB to 9.5 dB were tested and gave similar SRI sensitivity comprised in a range of about 538 nm/RIU ± 4 nm/RIU. The vertical deviations from each data point to the fitted line are measured to define the root mean square (rms) of the error on the wavelength and thus define the SRI uncertainty. The results indicate a rms refractive index uncertainty of 5×10^{-5}. The measurement errors on the SRI (1.2×10^{-5}) and on the wavelength (1.25 pm) are reported in Fig. 8 but do not appear clearly because the errors are very low in comparison to the full range of SRI.

The possibility of automation, thanks to the algorithm developed to treat the amplitude spectra, remains the main feature of this demodulation technique, with the added benefit that a single algorithm is used to identify both the absolute value of the SRI over a wide range (1.32–1.39 RIU) and very small changes around that value. To improve further the degree of automation and so the processing speed, a modification of the setup described in Fig. 1 could be to use a polarizing beam splitter and a two port detector behind the SPR sensor as proposed in [15]. In doing so, we would be able to collect rapidly both orthogonal amplitude spectra and to obtain the deducted SRI in less than a few seconds.

4. Conclusions

In this paper, we have demonstrated the operating principle of an automated demodulation technique for a TFBG-SPR refractometer. The SRI value is deduced from the differential amplitude of corresponding resonance peaks near the plasmon attenuation for two orthogonal amplitude spectra. The method is automated, easy to implement and provides an absolute measurement of SRI over a full range of 1.32 to 1.39 RIU with a demonstrated uncertainty of at least 5×10^{-5}.

The authors acknowledge the Wallonia (Sensendo and Opti2Mat projects), as well as the Interuniversity Attraction Pole of the BelSPo photonics@be.

C. Caucheteur is supported by the Fonds de la Recherche Scientifique (FRS-FNRS). J. Albert is supported by the Canada Research Chairs program, National Sciences and Engineering Research Council of Canada (NSERC), and LxData.

References

1. A. Iadicicco, S. Campopiano, A. Cutolo, M. Giordano, and A. Cusano, "Refractive index sensor based on microstructured fiber Bragg grating," IEEE Photon. Technol. Lett. **17**, 1250–1252 (2005).
2. T. Guo, H.-Y. Tam, P. A. Krug, and J. Albert, "Reflective tilted fiber Bragg grating refractometer based on strong cladding to core recoupling," Opt. Express **17**, 5736–5742 (2009).
3. G. Laffont and P. Ferdinand, "Tilted short-period fiber-Bragg-grating induced coupling to cladding modes for accurate refractometry," Meas. Sci. Technol. **12**, 765–770 (2001).
4. C. Chan, C. Chen, A. Jafari, A. Laronche, D. J. Thomson, and J. Albert, "Optical fiber refractometer using narrowband cladding-mode resonance shifts," Appl. Opt. **46**, 1142–1149 (2007).
5. C. Caucheteur and P. Mégret, "Demodulation technique for weakly tilted fiber Bragg grating refractometer," IEEE Photon. Technol. Lett. **17**, 2703–2705 (2005).
6. T. Erdogan and J. E. Sipe, "Tilted fiber phase gratings," J. Opt. Soc. Am. **13**, 296–313 (1996).
7. T. Guo, C. Chen, A. Laroche, and J. Albert, "Power-referenced and temperature-calibrated optical fiber refractometer," IEEE Photon. Technol. Lett. **20**, 635–637 (2008).
8. Y. Y. Shevchenko and J. Albert, "Plasmon resonances in gold-coated tilted fiber Bragg gratings," Opt. Lett. **32**, 211–213 (2007).
9. Y. Y. Shevchenko, C. Chen, M. A. Dakka, and J. Albert, "Polarization-selective grating excitation of plasmons in cylindrical optical fibers," Opt. Lett. **35**, 637–639 (2010).
10. T. Allsop, R. Neal, S. Rehman, D. J. Webb, D. Mapps, and I. Bennion, "Generation of infrared surface plasmon resonances with high refractive index sensitivity utilizing tilted fiber Bragg gratings," Opt. Express **17**, 16505–16517 (2007).
11. M. Piliarik and J. Homola, "Surface plasmon resonance (SPR) sensors: approaching their limits?," Appl. Opt. **46**, 5456–5460 (2009).
12. R. Naraoka and K. Kajikawa, "Phase detection of surface plasmon resonance using rotating analyzer method," Sensors Actuators B Chem. **107**, 952–956 (2005).
13. K.-H. Chen, J.-H. Chen, S.-W. Kuo, T.-T. Kuo, and M.-H. Lai, "Non-contact method for measuring solution concentration using surface plasmon resonance apparatus and heterodyne interferometry," Opt. Commun. **283**, 2182–2185 (2010).
14. C. Caucheteur, Y. Shevchenko, L. Shao, M. Wuilpart, and J. Albert, "High resolution interrogation of tilted fiber grating SPR sensors from polarization properties measurement," Opt. Express **19**, 1656–1664 (2011).
15. C. Caucheteur, Y. Shevchenko, L. Shao, P. Mégret, and J. Albert, "Demodulation technique for plasmonic fiber grating sensors using orthogonally polarized light states," in *Proceedings of the 21st Optical Fiber Sensors Conference* (2011), paper No. 7753-354.
16. L. Shao, Y. Shevchenko, and J. Albert, "Intrinsic temperature sensitivity of tilted fiber Bragg grating based surface plasmon resonance sensors," Opt. Express **18**, 11464–11471 (2010).